Applied Clay Science 232 (2023) 106791

Contents lists available at ScienceDirect

Applied Clay Science

journal homepage: www.elsevier.com/locate/clay

Research Paper

Hydrothermally treated vermiculites: Ability to support products for CO_2 adsorption and geological implications

Celia Marcos [a,*], Ayoub Lahchich [a], Pedro Álvarez-Lloret [a,b]

[a] Department of Geology and Enrique Moles Institute, University of Oviedo, Oviedo 33005, Spain
[b] Department of Mineralogy and Petrology, University of Granada, Granada 18071, Spain

ARTICLE INFO

Keywords:
Vermiculite
Expansion treatment
Hydrothermal treatment
Vermiculitization
Carbon dioxide

ABSTRACT

The proposal of this research was to obtain products with higher porosity and specific surface area than the raw vermiculite for its possible application as a support material for CO_2 adsorption. In addition, it was proposed to analyze the possible geological implications of the products resulting from the hydrothermal treatment of vermiculites in relation to their genesis. Hydrothermal treatment in the presence of CO_2, at low temperature and pressure conditions, was carried out in two vermiculites from Uganda and China, with different behavior to thermal exfoliation and microwave irradiation. The untreated and treated samples were characterized by several techniques: X-ray diffraction (XRD) for obtaining the mineral composition; thermogravimetry (TG - DTG) for analyzing the thermal behavior; and BET isotherms for obtaining textural parameters. In addition, the hydrothermal solutions were characterized by the pH and the measuring of the lixiviated elements with inductively coupled plasma mass spectrometry (ICP-MS). Vermiculite can be a suitable support for CO_2 adsorbents, based on the S_{BET} and Q_m values, and it is susceptible to carbonation. The hydrothermal treatment produced water loss in the expanded vermiculites by CO_2 replacement; as consequence, amorphization occurred in the purer Ugandan sample, and vermiculitization occurred in the less pure sample from China.The vermiculitization process indicates that the geological origin of vermiculite may be hydrothermal from phlogopite.

1. Introduction

During the last decades, the increase in harmful emissions to the atmosphere has been related to the intensive use of fossil fuels in sectors such as industry, construction and transportation. These gaseous emissions have caused the concentration of some compounds, such as hydrogen sulphide (H_2S), ammonia (NH_3), carbon monoxide (CO), sulphur dioxide (SO_2) and/or nitrogen oxides (NO_x), with potential toxic effects in interaction with various atmospheric phenomena. Therefore, this increase is considered the main cause of global warming, climate change and acid rain, leading to these effects having detrimental consequences for health and the environment (Yang et al., 2008).

One of the most pressing challenges facing humans today is global warming, where the increasing concentration of CO_2 in the atmosphere plays a key role in this environmental problem (Wang et al., 2014; Harvey et al., 2017). Carbon dioxide is the most important greenhouse gas in the atmosphere, being responsible for the main climate warming effect. According to NASA, the amount of CO_2 in Earth's atmosphere was about 418 ppm (ppm) in May 2022, constituting 50% more than in the beginning of the industrial era between 1750 and 1800 (NASA Global Climate Change, 2022). Scientists estimate that before human industrial activity, CO_2 concentrations were about 270 ppm by volume (Collins et al., 2013; Lan et al., 2020).

Several alternatives have been developed so far to mitigate CO_2 emissions, such as the use of hydrogen and the renewable energies transition (Sordakis et al., 2018; Kabir et al., 2018). However, currently the life-style is mostly dependent on fossil fuels, which slows down the shift to the use of other sources of energy production. Therefore, one of the most promising and effective ways to mitigate CO_2 emissions with less impact consists of CO_2 capture and storage (Rahman et al., 2017). Carbon dioxide capture and storage (CCS) is a set of technologies designed to prevent the release of CO_2 and its permanent storage in order to greatly reduce CO_2 emissions. In this process, some authors have pointed out that CO_2 capture is the most costly step (between 50 and 90% of the overall cost) so the main efforts are directed to the development of technologies that enable more efficient CO_2 capture mechanism (Pera-Titus, 2014). At present, the most widely used technologies in CO_2 capture propose the application of cryogenic distillation,

* Corresponding author.
E-mail address: cmarcos@uniovi.es (C. Marcos).

https://doi.org/10.1016/j.clay.2022.106791
Received 3 September 2022; Received in revised form 29 November 2022; Accepted 30 November 2022
Available online 15 December 2022

membrane purification and adsorption (Choi et al., 2018). Among them, the most advanced technology in CO_2 capture is its adsorption by means of amines, achieving excellent performance (Chouikhi et al., 2019). Although this methodology also presents several drawbacks related to its high energy requirements needed in the regeneration stage, as well as, the high corrosion of the amine species (Chouikhi et al., 2019).

The use of adsorbent materials to capture CO_2 has emerged as an alternative to the technologies indicated above due to their reduced energy demands and simpler operating conditions. Most efforts are focused on the search and development of adsorbents with high adsorption capacity and selectivity for CO_2. Various porous materials have been evaluated as potential molecular sieves for CO_2 capture: graphenes (Haque et al., 2017), zeolites (Li et al., 2008), porous silica (Sanz-Pérez et al., 2018) or activated carbon (Pevida et al., 2008). Thus, clay minerals have become an alternative due to their excellent adsorption and catalysis behavior (Bergaya and Lagaly, 2013). These factors, together with their high availability and stability, makes them potential adsorbents to be used in CO_2 capture processes. Previous studies have confirmed that clay-group minerals, such as montmorillonite, are materials that can equally be used as amine supports (Wang et al., 2014; Harvey et al., 2017), substances with high CO_2 adsorption capacity (Atilhan et al., 2016) as previously stated.

Vermiculite is a low-cost phyllosilicate, which, due to its characteristics of stability, safety, abundant reserves, easy exfoliation, high porosity and specific surface area (Midgley and Midgley, 1960; Couderc and Douillet, 1973; Hillier et al., 2013; Marcos, 2020) make it a suitable support for CO_2 adsorbents, such as amines (Zhang et al., 2020) or calcium oxide (Pereira et al., 2022). On the other hand, vermiculite could be susceptible to carbonation like other silicates (Lackner et al., 1997). The experimental carbonation process (Lackner et al., 1997; Seifritz, 1990) consists of pumping CO_2 gas into an agitated mixture of water and divalent metal-bearing silicates (such as vermiculite, magnesium silicate). The mixture is heated and subjected to controlled CO_2 gas pressure. The CO_2 reacts with the silicates via the aqueous solution and can lead to the formation of carbonate phases, such as magnesite, calcite or dolomite (Daval et al., 2009; Sanna et al., 2014). Later, the reaction solution is filtered and dried, resulting in a carbonate mineral that will remain stable over geological time periods, mimicking the natural alteration of silicates. In this process, it is a matter of having a mineral, source of magnesium hydroxide (e.g. vermiculite), which would react with CO_2 to produce magnesite ($MgCO_3$). This carbonate mineral, as a by-product of the reaction, can also have numerous industrial applications (i.e., construction material, animal feed, fertilizers, glass and paper manufacturing, etc.).

In summary, during a mineral carbonation process, atmospheric CO_2 can almost permanently adopt a solid form through chemical reactions with certain extracted minerals present in the Earth's crust. As a result of this capture process, the emission of CO_2 into the atmosphere would be limited by accumulating in reservoirs that would not require excessive monitoring and the associated risks would be very low. Furthermore, this direct transformation of CO_2 gas into solidified carbonates represents an industrially efficient route for its utilization, generating stable, inert, non-hazardous and profitable materials for its different uses.

In this work, two vermiculites from different provenance and with different behavior to thermal heating and microwave irradiation were treated hydrothermally in the presence of CO_2, at low temperature and pressure experimental conditions. The reaction products resulting were characterized by X-ray diffraction, thermogravimetry, and BET isotherms. In addition, the aqueous solutions were characterized by the pH measuring and inductively coupled plasma mass spectrometry. The transformations undergone by the investigated vermiculites subjected to physical and hydrothermal treatments may cause textural and structural changes in them. These alterations can also help us to reveal the possible hydrothermal origin of vermiculite from phlogopite in geological environment.

2. Materials and Methods

2.1. Materials

The vermiculite samples investigated were provided by the company Vermiculita y Derivados S.A. (Gijón, Spain). One comes from Uganda, and it has been labeled as V-U-20. The other comes from China and it has been labeled as V-CHG-20. The particle size of both vermiculites is <5 mm in diameter and the thickness varies from 0.5 to 1 mm. The Ugandan vermiculite is golden in color and the Chinese vermiculite is brownish green (Fig. 1).

Vermiculite from China, containing 3.92% of K_2O (Marcos et al., 2020), is less pure than that from Uganda, with 0.36% of K_2O (Marcos, 2022), according to the criteria considered within Velde (1978).

2.2. Methods

2.2.1. Experiments

To achieve the proposed objectives, three types of experiments were carried out using the raw vermiculites: high temperature thermal treatment, microwave irradiation treatment and hydrothermal treatment. The first two treatments were performed in order to expand the samples and compare the response with the raw and expanded samples.

To perform the high temperature thermal treatment to expand the samples a Carbolite CWF 12/23 type furnace was used. The furnace was first stabilized at a temperature of 900 °C. Then, the vermiculite sample was introduced and heated for 1 min, after which it was removed and allowed to cool at room temperature.

Fig. 2a and 2b shows images of the samples from Uganda and China expanded at 900 °C for 1 min. Figs. 2c and 2d show scanning electron microscope (SEM) images of the samples from Uganda and China expanded at 900 °C for 1 min. Samples were labeled as V-U-900 and V-CHG-900, respectively.

The microwave experiments were performed with a microwave oven (SHARP R64sT) operating at 2.45 GHz and 800 W. The raw Ugandan sample required 1 min of irradiation to expand, while the less pure Chinese sample required only 20 s. Samples were labeled as V-U-MW and V-CHG-MW, respectively. The appearance of the samples after irradiation is as shown in Figs. 3a and 3b and the SEM images of the vermiculite are shown in Figs. 3c and 3d.

Vermiculite-water-CO_2 interaction experiments were performed using a steel reactor (BR-100, Berghof) with a temperature-time controller (BTC-3000, Berghof) coupled to a pressure probe and gauge. The reactor includes a PTFE vessel inset (polytetrafluoroethylene, 75 mL total volume). Raw and expanded vermiculite samples (V-U-20, V-U-900, V-U-MW, V-CHG-20, V-CHG-900, V-CHG-MW) were used for the hydrothermal experiments. For each sample, approximately 1.50 g of vermiculite and 60 mL of distilled water were added to the PTFE vessel which was then inserted into the steel reactor and sealed using a mechanical system. Using an industrial CO_2 gas cylinder attached to the reactor, a flow of CO_2 was passed through for 3 min to displace the air content of the reactor vessel; the valves were then closed until a pressure of 10 bars was reached. Subsequently, the reactors were heated at 100 °C for 24 h with stirring at 200 rpm. At the end of the experimental time, the reactors were allowed to cool down to room temperature and the pressure valves were opened to expel the remaining CO_2 from the reactor. The content of the vessel was filtered using 0.2 μm membrane filter (Millipore) and once the solid was separated, it was dried at room temperature for 24 h. The dried vermiculite samples were labeled as V-U-20-24, V-U-900-24, V-U-MW-24, V-CHG-20-24, V-CHG-900-24, V-CHG-MW-24, respectively. The aqueous solutions were preserved in plastic conical tubes (Falcon model) for subsequent chemical analysis. The dried samples were weighed by precision microbalance to obtain the difference in weight with respect to the initial one. All the samples were subsequently characterized (see below for further details). The appearance of the dried vermiculite samples after hydrothermal

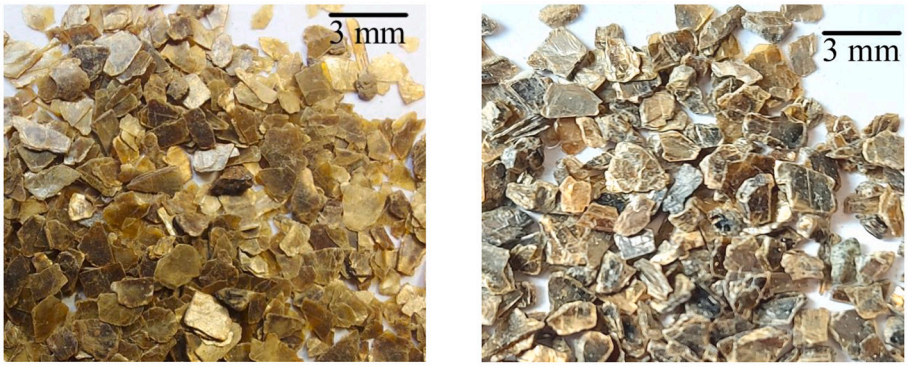

Fig. 1. Appearance of the raw vermiculites: (a) Ugandan vermiculite, (b) Chinese vermiculite.

treatment is shown in Fig. 4.

2.2.2. Characterization

The pH of the distilled water and the hydrothermal solutions at room temperature after separation of the solid phase was measured with a CRISON BASIC 20 peachimeter, using a glass electrode (Metrohm) calibrated with three standard solutions (pH = 4.01, 7.01 and 10.01 at 25 °C) with ±0.01 uncertainty.

Subsequently, an Agilent Technologies "HP 700" model ICP- MS has been used to know if there was leaching of cations from the vermiculite during the hydrothermal treatment.

An Entris precision balance (Sartorius) was used to weigh the samples pre and post hydrothermal treatment (weight loss).

Later, raw and treated vermiculites were characterized by means of different instrumental techniques allowing the follow-up and evolution of the products of the previously described experiments (i.e., high temperature expansion, microwave irradiation expansion and hydrothermal reaction treatments).

The X-ray diffraction technique was used with the crystalline powder method to identify the crystalline phases of the treated samples. The vermiculite samples, 0.5 g of each, were previously ground in an agate mortar to obtain the diffractograms. An X-ray diffractometer PHILIPS X'PERT PRO was employed using the following instrumental conditions: 40 mA and 45 kV (Cu-Kα radiation; λ = 1.5418 Å), 2θ 5–70, 2θ scan step of 0.007° and a counting time of 1 s per step.

Thermogravimetric analyses were performed between 25 °C and 1000 °C using a Mettler Toledo Stare System AG-TGA/SDTA851e thermobalance with a heating rate of 10 °C/min. The total mass loss was determined gravimetrically by heating the samples in an inert atmosphere (N_2) at 1000 °C in a muffle furnace. The initial mass of the sample was about 20 mg.

Textural parameters (i.e., specific surface area and porosity) of the powdered samples were determined with the ASAP 2020 equipment (Micrometrics) under the following conditions: Nitrogen adsorption at 77.35 K, with σ_m (N_2) of 0.162 nm^2, unrestricted evacuation of 30.0 mmHg, vacuum pressure of 10 μm Hg, evacuation time of 1 h, and the temperature of sample evacuation prior to N_2 adsorption measurements was 22 °C. The data were recorded with equilibration times (p/p_0 between 0.001 and 1.000) between 50 s and 25 s and a minimum equilibrium delay of 600 s at $p/p_0 \geq 0.995$.

3. Results and discussion

3.1. pH values of the hydrothermal solutions

The pH of the hydrothermal solutions after filtration of the samples (Table 1) increased compared with the pH of the distilled water (7.2) used in the hydrothermal experiments.

The pH variation of hydrothermal solutions is related to the dissolution of CO_2 in water, which is a Lewis acid, and it hydrolyzes water giving protons to the medium, according to the process $CO_2(aq) + H_2O$ (l) $HCO_3^-(aq) + H^+(aq)$, making more acidic the pH of the water. The observed pH increase into slightly alkaline values at the end of the hydrothermal experiment suggests that after an initial period of vermiculite dissolution by acidic conditions, OH^- groups are released in the aqueous solution. The replacement of CO_2 by structural water and OH^- groups would be the cause of the presence of these groups in the solution, in a similar way to the entry of alcohol into vermiculite (Marcos and Rodriguez, 2016, 2017). This effect on pH is accompanied by the leaching of alkaline-earth metals into the aqueous solutions and the alteration of vermiculite properties at the end of the hydrothermal experiments (see below for details).

3.2. ICP-MS analyses of the hydrothermal solutions

The semi-quantitative analysis of the main elements obtained by ICP-MS analyzed in the aqueous solutions resulting from the filtration of the hydrothermally treated vermiculites is presented in Table 2. The decreasing order of leaching of the elements from the vermiculites was as follows Na > Si > Cl > Mg > K > Ca. The C content comes from the CO_2 dissolved in the water.

3.3. Mass percentage variation of the hydrothermal treatment samples

The mass percentage of the pre and post hydrothermal treatment samples and the pressure before and after hydrothermal treatment are presented in the Table 3. The mass loss was of 6.7% except in samples V-U-900-24 and V- CHG −900-24, which was 0.7% and 13.3%, respectively.

The mass loss of hydrothermally treated samples is due to the leaching of vermiculite elements such as sodium, silicon, magnesium, potassium and calcium and the water loss. As a result, the pressure decreased during hydrothermal treatment in all cases, more homogeneously in the samples from China than in those from Uganda.

3.4. X-ray diffraction analyses

The X-ray diffraction patterns of the raw and treated samples from Uganda (Fig. 5) show that the reflections of all of them correspond to those of vermiculite (JCPDs card 16–613), the *d*-value of 14.56 Å correspond to the most characteristic reflection 002 of the Ugandan raw vermiculite. In the XRD pattern of the V-U-MW sample (inset of Fig. 5) the reflection with *d*-value of 12.71 Å corresponds to an interstratified. In the V-U-900 the *d*-values of 10.04 and 9.40 Å correspond to dehydrated phases. The *d*-value of the reflection 002 of the V-U-20 sample decreases 0.08 Å in the V-U-20-24 sample, and 0.17–0.18 Å in the V-U-

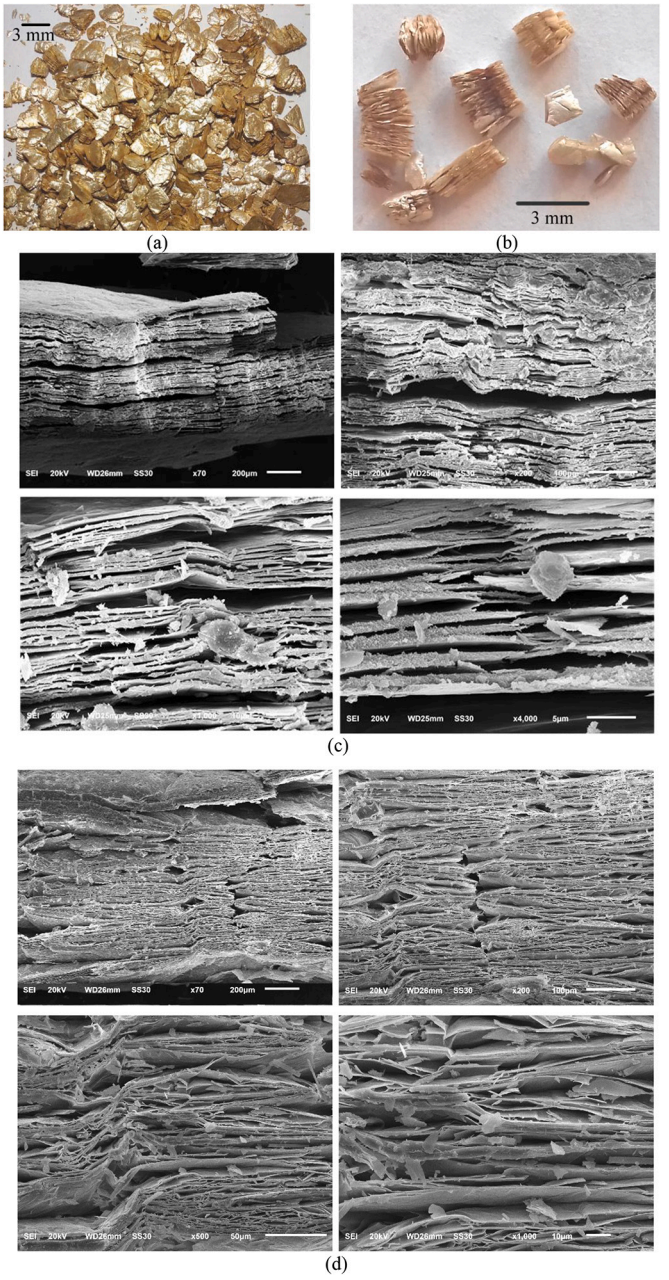

Fig. 2. Images of vermiculite samples expanded at 900 °C for 1 min from Uganda (a) and China (b). SEM images of vermiculite samples expanded at 900 °C for 1 min from Uganda (c) and China (d).

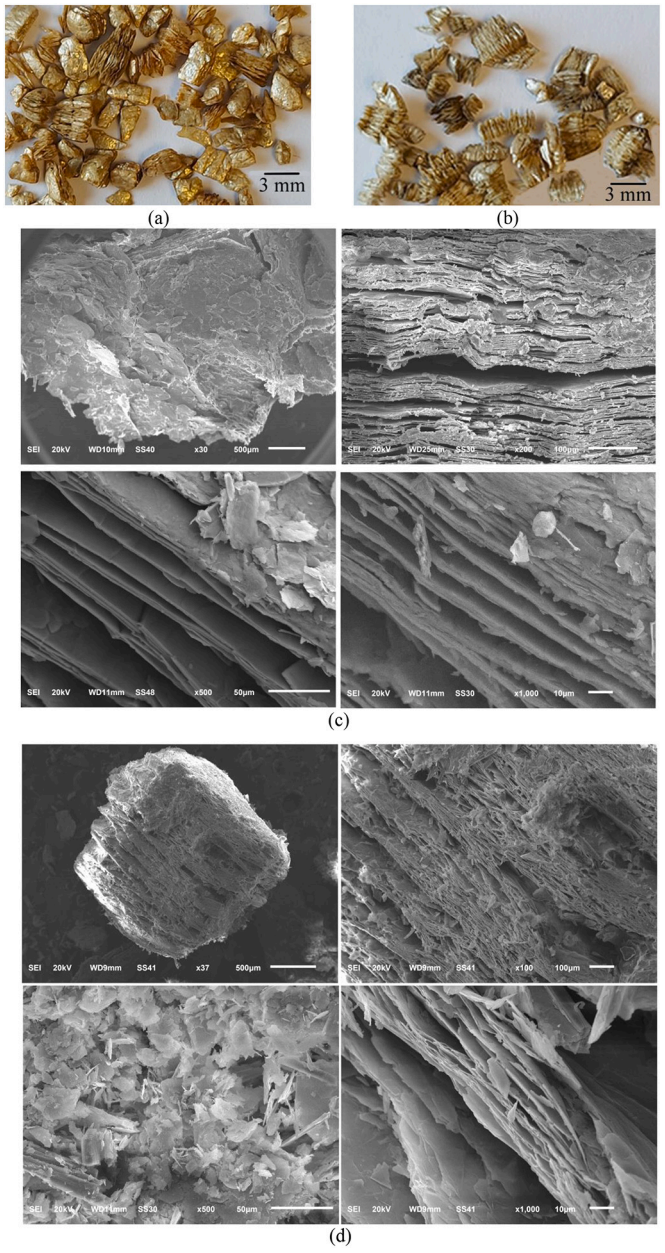

Fig. 3. Images of vermiculites samples expanded by microwave irradiation: (a) Uganda and (b) China. SEM images of the vermiculite samples expanded by microwave: (c) Uganda and (d) China.

MW and V-U-900 samples. The intensity of the reflection 002 hardly decreases in the V-U-MW sample, but in the V-U-900 sample the decreasing is very drastic. The intensity decreasing of the reflection 002 of the V-U-20-24, V-U-MW-24 and V-U-900-24 samples is also notable.

The X-ray diffraction spectra of the raw sample and the treated samples from China are presented in Fig. 6. Detected reflections correspond to vermiculite (V) (JCPDs card 10–418), hydrobiotite (JCPDs card 13–465) and/or an interstratified (I) and phlogopite (Phl) (JCPDs card 16–344). The similarities and differences among the patterns can be seen more clearly in the inset of Fig. 6: The V-CHG-20 and V-CHG-MW samples are similar. The reflections corresponding to sample V-CHG-900 coincide with those of phlogopite (JCPDs card 16–344). Phlogopite practically disappears in the V-CHG-20-24 and V-CHG-MW-24 samples. In the V-CHG-900-24 sample vermiculite appeared again. This vermiculitization process by hydrothermal treatment of less pure samples such as the one from China shows that vermiculite can be obtained from phlogopite by hydrothermal processing at low temperature and pressure, in the presence of CO_2, corroborating the experiments of Roy and Romo (1957) and the idea of Marcos (2020) on treatments involving water loss in vermiculites would help to reveal data related to their hydrothermal origin.

XRD revealed interstratified phases in the Chinese raw vermiculite, unlike the Ugandan raw vermiculite. According to Marcos (2020), this is because the former has a higher K^+ content and lower water content (see Table 4) than the Ugandan vermiculite. As a consequence, the behavior of both samples to heat and hydrothermal treatments was different, observing some alterations at the structural level. On the one hand, the Ugandan vermiculite heated abruptly to 900 °C dehydrated and began to transform into enstatite (Marcos et al., 2009), which was evidenced in Fig. 5 by reflection (221) at 3.14 Å (JCPDS card 19–606). The hydrothermally treated samples V-U-20-24, V-U-MW-24 and V-U-900-24

Fig. 4. Appearance of dry vermiculite samples from Uganda (a) and China (b) after hydrothermal treatment.

Table 1
pH values of the hydrothermal solutions at $P = 10$ bar and $T = 100$ °C at the end of the experiments.

Hydrothermal solution	pH
V-U-20-24	8.54
V-U-MW-24	8.44
V-U-900-24	8.95
V-CHG-20-24	8.92
V- CHG -MW-24	9.31
V- CHG −900-24	9.26

Table 2
Semi-quantitative analysis obtained by ICP-MS of the measured main elements (ppm) in the solutions of hydrothermally treated vermiculites in the presence of CO_2.

Samples		C	Na	Si	Mg	Cl	K	Ca
	Distilled H_2O	50	<1	<1	0	6	<1	0
Hydrothermal solutions after filtering the samples	V-U-20-24	2641	191	32	10	10	1	3
	V-U-900-24	819	18	10	5	9	2	1
	V-U-MW-24	1513	8	7	2	8	<1	1
	V-CHG-20-24	620	30	8	<1	8	2	2
	V-CHG-900-24	2416	9	9	2	7	6	1
	V-CHG-MW-24	380	17	5	<1	7	1	<1

Table 3
Mass (g) of the pre and post hydrothermal treatment samples and the pressure before and after hydrothermal treatment.

Samples	Mass (g)		Mass loss (%)	Pressure (bar)	
	Pre-treatment	Post-treatment		Pre-treatment	Post-treatment
V-U-20-24	1.504	1.403	6.7	10	9
V-U-MW-24	1.504	1.427	6.7		7
V-U-900-24	1.505	1.497	0.7		6.5
V-CHG-20-24	1.505	1.426	6.7		8
V-CHG-MW-24	1.511	1.390	6.7		8
V-CHG-900-24	1.522	1.296	13.3		8

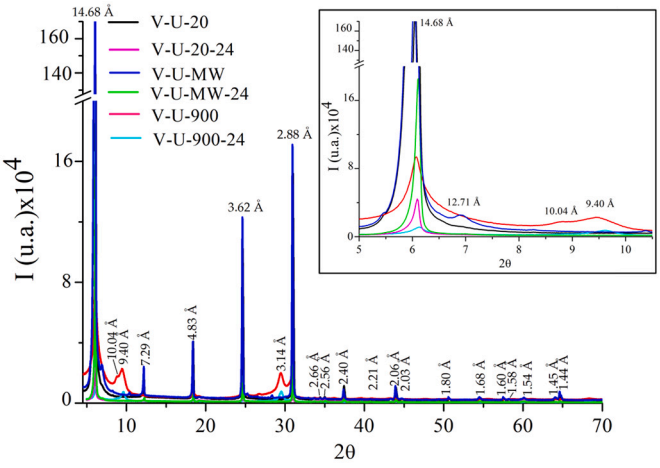

Fig. 5. X-ray diffraction patterns of the raw and treated vermiculites from Uganda. All reflections correspond to those of the vermiculite. The inset of the figure shows the decrease in intensity suffered by the 002 reflection of the treated samples in relation to the raw sample, except for the sample irradiated with microwaves, as a consequence of dehydration.

suffered a decrease in intensity, the cause of which is outlined below. On the other hand, vermiculite from China transformed into phlogopite mica with abrupt heating, according to Marcos et al. (2009); the samples V-CHG-20-24 and V-CHG-MW-24 increased slightly in intensity and V-CHG-900-24 transformed to vermiculite, with hydrothermal treatment.

The loss of intensity of the reflections of the expanded samples of Uganda and China is due to the water loss according to the mechanism explained by Hillier et al. (2013). The decrease in intensity of the DRX reflections of the hydrothermally treated samples can be explained by a loss of structural H_2O due to the displacement by CO_2 entry.

Although there are ambiguities regarding the geological origin, hydrothermal and/or supergene, of the vermiculites, most and possibly all macroscopic vermiculite and interstratifications of vermiculite and other phases (mica, chlorite) are believed to have a supergene origin (Bassett, 1961; Toksoy-Koksal et al., 2001). The changes suffered by vermiculites due to hydrogen peroxide treatment and ionic metal exchange, with water gain, could point to this origin (Marcos, 2020), corroborating both the field and laboratory evidence in early times (Bassett, 1961). Some aspects observed in the transformations caused by treatments with water loss could coincide with field observations (Churchman and Lowe, 2012; Mohammed and Al-Mashaikie, 2018).

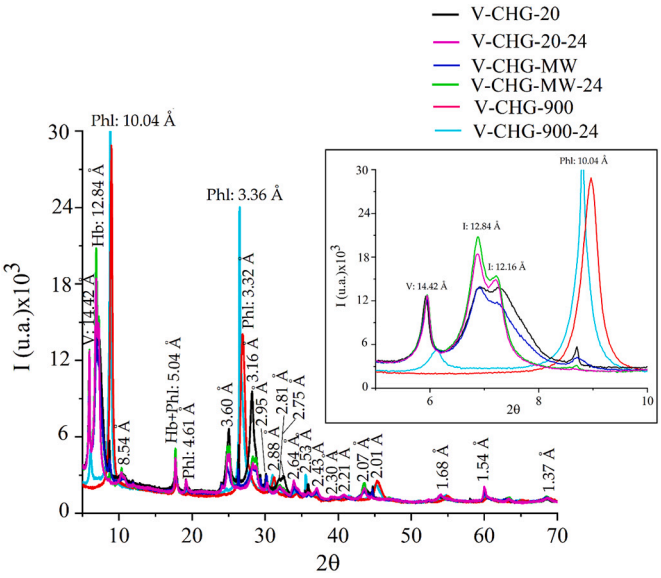

Fig. 6. X-ray diffraction patterns of raw and treated vermiculites from China. Reflections correspond to those of vermiculite (V), hydrobiotite and/or an interstratified (I) and phlogopite (Phl). The inset of the figure shows the similarities and differences among the patterns.

Table 4
Water and mass loss obtained by TG analyses in the range of 25 to 1100 °C of the samples untreated and treated from Uganda and China.

Samples	H_2O loss (%) 1st step	Mass loss (%) 2nd step
V-U-20	15.6	4.5
V-U-20-24	13.3	6.1
V-U-900	6.4	3.6
V-U-900-24	4.5	3.9
V-U-MW	14.2	4.0
V-U-MW-24	14.1	5.6
V-CHG-20	8.5	4.9
V-CHG-20-24	8.6	4.8
V-CHG-900	3.2	0.0
V-CHG-900-24	1.5	3.5
V-CHG-MW	7.8	5.0
V-CHG-MW-24	8.5	4.7

3.5. Thermogravimetric analyses

The thermal behavior of the samples from Uganda and China is shown in Figs. 7 and 8, respectively. The TG curves (Figs. 7a and 8a, respectively) show that the decomposition of the samples takes place in two steps. The first step extends from 25 to about 250 °C (endothermic peak) and is due to the loss of adsorbed water on the surface and/or localized in the interlayer space (see e.g., de la Calle and Suquet, 1988; Argüelles et al., 2010). In a second step, at temperatures above 800 °C, an additional mass loss is observed. This mass loss (exothermic peak) is due to recrystallization into new phases or to a transformation process associated with the dehydroxylation of OH^- anions in the octahedral layer (see e.g., de la Calle and Suquet, 1988; Marcos et al., 2009). The mass loss in both stages is equal to or <20% (Table 4). The difference between the TG curves of Ugandan and Chinese vermiculites is due to water loss, which is almost twice as high in the former as in the latter. According to Marcos (Marcos, 2020) the structural water loss cause crystallinity loss of vermiculite and therefore structural disorder increase. In the case of V-CHG-900 and V-CHG-900-24, water loss is very low, mainly in the latter, causing the appearance of the vermiculite phase, corroborated by XRD. These changes give light to their geological origin related to hydrothermal processes.

The most significant difference is presented by sample V-CHG-900-24 in the DTG curve with the presence of a very accentuated peak at 650 °C due to transformation processes associated with the dehydroxylation of OH^- anions in the octahedral sheet (de la Calle and Suquet, 1988; and Marcos et al., 2009) and related to the vermiculite phase identified by X-ray diffraction in this sample.

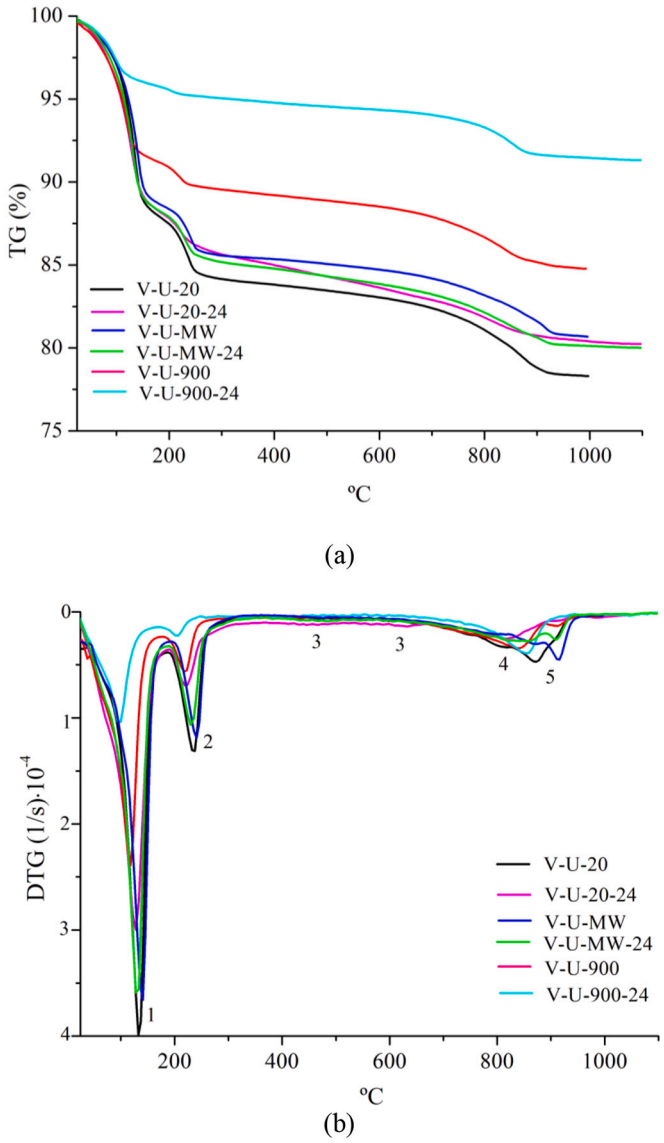

Fig. 7. TG (a) and DTG (b) curves of Uganda samples. Note: 1 - adsorbed surface water loss; 2 - interlayer water loss and interlayer cation-bound water; 3 - loss of hydroxyls; 4 - decomposition of CO_2; 5 - recrystallization.

Five different steps can be observed in the DTG curves. The first step, ranging from approximately 50 to 150 °C, is due to the loss of surface adsorbed water. In a second step, at temperatures above 200 °C, a loss of the interlayer water and water bound to the interlayer cations is observed. The third step, at temperatures between 550 and 650 °C, is due to the loss of hydroxyls. The fourth step is due to CO_2 decomposition (Inguanzo et al., 2001; Pereira et al., 2022) and the fifth step, at temperatures above 850 °C, due to phase recrystallization. The most significant difference is presented by sample V-CHG-900-24 with the presence of a very pronounced peak at 650 °C related to dehydroxylation of OH^- anions in the octahedral sheet (de la Calle and Suquet, 1988; and Marcos et al., 2009) and related to the vermiculite phase identified by X-ray diffraction in this sample. This peak is missing in Ugandan vermiculite.

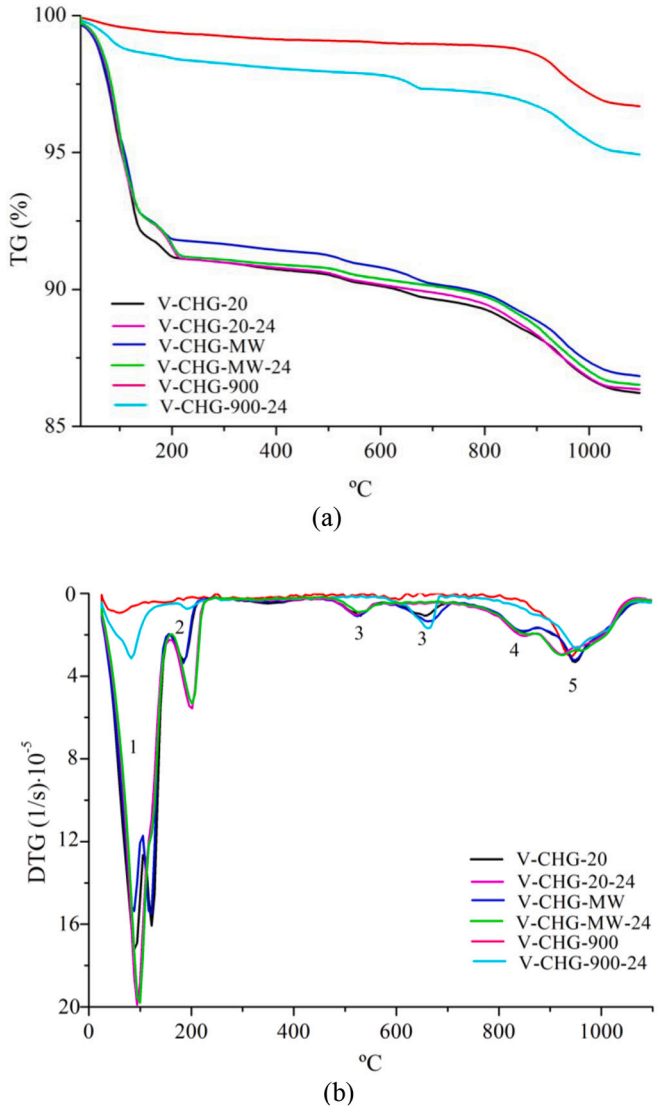

Fig. 8. TG (a) and DTG (b) curves of China samples. Note: 1 - adsorbed surface water loss; 2 - interlayer water loss and interlayer cation-bound water; 3 - loss of hydroxyls; 4 - decomposition of CO_2; 5 - recrystallization.

3.6. Textural parameters

The nitrogen adsorption-desorption isotherms from Uganda vermiculites are shown in Fig. 9a for the V-U-20 and V-U-20-24 samples, in Fig. 9b for the V-U-900 and V-U-900-24 samples and in Fig. 9c for the V-U-MW and V-U-MW-24 samples. The nitrogen adsorption-desorption isotherms from China vermiculites are shown in Fig. 10a for the V-CHG-20 and V-CHG-20-24 samples, in Fig. 10b for the V-CHG-900 and V-CHG-900-24 samples and in Fig. 10c for the V- CHG-MW and V-CHG-MW-24 samples. The nitrogen adsorption-desorption isotherms of the untreated and treated vermiculites from Uganda and China correspond to type IV, based on IUPAC classification, showing characteristics of mesoporous solids (Thommes et al., 2015). The slight H3 hysteresis exhibited by the samples is characteristic of layered particles, such as phyllosilicate group minerals, including vermiculite (Thommes et al., 2015). The specific surface area (S_{BET}), adsorption capacity (Q_m), total pore volume (V_p), pore size (nm), BET constant (C), and correlation coefficient (R^2) values obtained from the adsorption-desorption experiments are shown in Table 5. The specific surface area (S_{BET}) was measured using the BET mathematical model. The total pore volume (Vp) refers to the volume occupied by the adsorbate within the

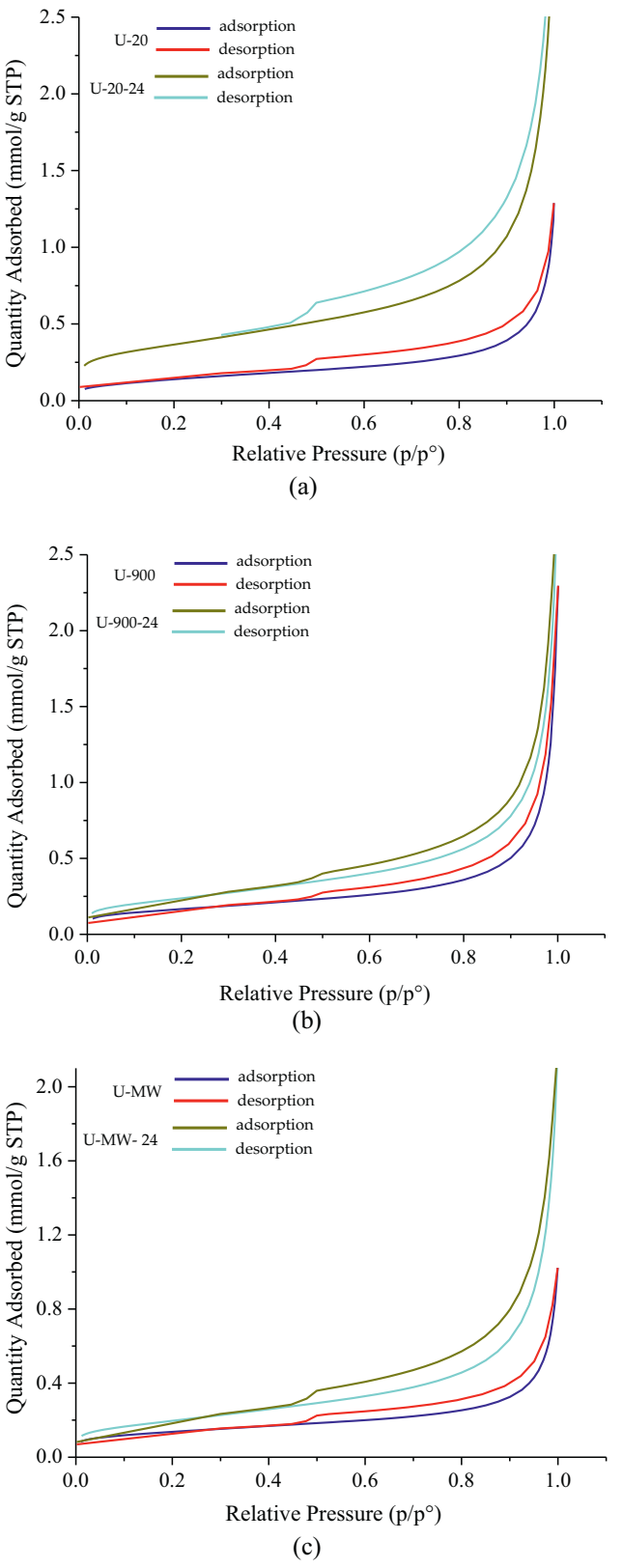

Fig. 9. Nitrogen adsorption-desorption isotherms of raw and treated vermiculites from Uganda at 20 °C (a), 900 °C (b) and microwave irradiated (c).

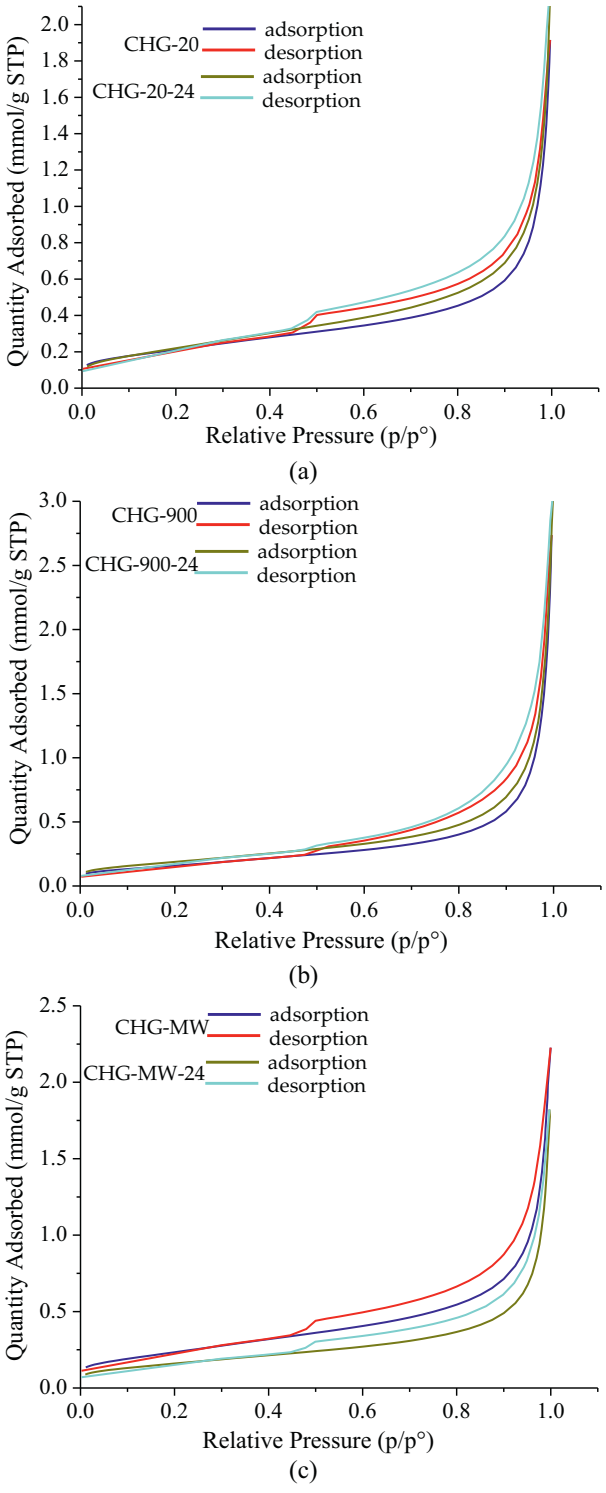

Fig. 10. Nitrogen adsorption-desorption isotherms of raw and treated vermiculites from China at 20 °C (a), 900 °C (b) and microwave irradiated (c).

adsorbent at a given pressure (usually close to $p/p_0 = 1$). The Vp expresses the volume occupied by the pores in a unit mass of solid and is expressed as mmol/g. The pore size distribution consists of expressing the pore volume versus the pore size to which it is ascribed. The model used in this work has been the Barret-Joyner-Halenda (BJH) model (Barrett et al., 1951), which is applied only to type IV isotherms, being the most used for the calculation of pore size distributions in the mesopore range (2–50 nm), In addition, this pore size calculation has been

Table 5
Specific surface area (S_{BET}), adsorption capacity (Q_m), pore volume (V_p), BET constant (C) and correlation coefficient (R^2) of nitrogen adsorption-desorption measurements for raw and treated vermiculites.

Sample	S_{BET} (m^2/g)	Q_m (mmol/g STP)	V_p (mmol/g STP)	Pore size (nm)	C	R^2
V-U-20	11.7 ± 0.1	0.12	0.005	2.93	55.1	0.9999
V-U-20-24	29.1 ± 0.1	0.30	0.0005	1.73	186.6	0.9999
V-U-900	13.2 ± 0.0	0.14	0.06	2.52	184.7	0.9999
V-U-900-24	19.2 ± 0.0	0.20	0.0003	2.11	106.8	0.9999
V-U-MW	11.0 ± 0.0	0.11	0.02	3.24	168.4	0.9999
V-U-MW-24	15.5 ± 0.1	0.16	0.002	4.00	133.1	0.9998
V-CHG-20	17.2 ± 0.1	0.18	0.0004	2.38	93.0	0.9999
V-CHG-20-24	18.1 ± 0.2	0.19	0.0004	2.29	70.0	0.9992
V-CHG-900	13.1 ± 0.1	0.13	0.09	2.62	76.3	0.9999
V-CHG −900-24	15.2 ± 0.1	0.16	0.0002	2.43	104.3	0.9997
V-CHG-MW	19.2 ± 0.2	0.20	0.0005	2.65	80.4	0.9995
V-CHG-MW-24	13.3 ± 0.1	0.14	0.05	2.50	58.5	0.9999

carried out considering the Faass correction (Faass, 1981), which adjusts for the change in thickness of the multilayer during the intervals in which the cores are not emptied, allowing to obtain a more accurate pore distribution. The C values of the investigated untreated and treated samples, ranging between 55 and 187 confirmed the validity of the BET method. The C values higher up to 150 of are generally associated with either adsorption on high-energy surface sites or the filling of narrow micropores. The C values lower than to 50 indicate there is then an appreciable overlap of monolayer and multilayer adsorption and the precise interpretation of nm is questionable (Thommes et al., 2015).

The S_{BET} value of the raw sample from China is much lower than that of the raw sample from Uganda, while the Vp value and pore size is slightly lower. The S_{BET} values are, in general, higher in the hydrothermally treated samples than in the non-hydrothermally treated ones, with the exception of sample V-CHG-MW-24. The same trend is observed with the Q_m value. The R^2 values for both samples that provide the goodness of fit are close to 1.

In Ugandan vermiculite, S_{BET} and Q_m values increased in hydrothermally treated samples (V-U-20-24, V-U-900-24 and V-U-MW-24) relative to those not hydrothermally treated (V-U-20, V-U-900 and V-U-MW). Conversely, V_p values decreased in the hydrothermally treated samples. Pore size decreased in the hydrothermally treated raw sample and 900 °C heated samples (V-U-20-24 and V-U-900-24) relative to the non-hydrothermally treated (V-U-20 and V-U-900); but increased in the hydrothermally treated microwave irradiated sample (V-U-MW-24) relative to the non-hydrothermally treated (V-U-MW-24).

In vermiculite from China, S_{BET} values increased in the hydrothermally treated raw and 900 °C heated samples (V-CHG-20-24 and V-CHG-900-24) relative to the non-hydrothermally treated (V-CHG-20 and V-CHG-900), but in vermiculite from Uganda decreased in the hydrothermally treated microwave irradiated sample (V-U-MW-24) relative to the non-hydrothermally treated (V-U-MW-24). The same trend is observed with the Q_m values. The V_p value was the same in the untreated (V-CHG-20) and hydrothermally treated (V-CHG-20-24) raw sample, but decreased in the hydrothermally treated sample heated to 900 °C (V-CHG-900-24) relative to the untreated (V-CHG-900) while increased in

the hydrothermally treated microwave irradiated (V-CHG-MW-24) relative to the non-hydrothermally treated (V-CHG-MW-24). Pore size values decreased in hydrothermally treated samples relative to untreated samples.

The differences in the BET results in the investigated samples seem to be related to the transformation or modification of the vermiculites by the loss of structural water due to exfoliation by physical treatments, high temperature heating and microwave irradiation.

Vermiculites are minerals that can be hydrothermally modified in such a way that their textural properties improve, increasing the specific surface area, which could increase therefore the CO_2 adsorption capacity. In relation to the S_{BET} and Q_m values, the products proposed for CO_2 adsorption are the raw vermiculite from Uganda and China after hydrothermal treatment at low temperature and pressure in the presence of CO_2. Between both, the samples from Uganda, which are compositionally purer, would behave better than those from China for use as support for other organic compounds, such as amines, with the ability to absorb CO_2.

4. Conclusions

In conclusion, the transformations undergone by the investigated commercial vermiculites subjected to physical (high temperature and microwave irradiation) and chemical (hydrothermal) treatments have caused compositional, textural and structural changes in them. These alterations have also allowed giving light on the possible hydrothermal origin of vermiculite from phlogopite.

The following specific conclusions can be drawn: 1) Mass of the raw and expanded vermiculites decreased after hydrothermal treatment as a consequence of the lixiviation of cations such as sodium, silicon or magnesium and the replacement of H_2O by CO_2. 2) pH of the hydrothermal solution of vermiculite increased due to the presence of OH^- groups in the vermiculite because of the replacement of CO_2 by structural water and these OH^- groups. 3) Water loss caused crystallinity loss of vermiculite and structural disorder increase 4) The hydrothermal treatment caused amorphization in purer expanded samples like Uganda and vermiculitization in expanded samples less pure such as China. This last fact is very important because it shows that the geological origin of vermiculite can be hydrothermal from phlogopite. 5) The most suitable vermiculites as supports for CO_2 adsorption are the hydrothermally treated raw samples, according to the S_{BET} and Q_m values.

The research presented here suggests using the hydrothermal treatment to increase the porosity of the vermiculite by a partial dissolution of its lamellae, favoring that these structures can act as a molecular sieve trapping the CO_2 molecules. On the other hand, it could be checked whether by means of hydrothermal treatment with acid solution and at higher pressure and temperature than the one used in this work, the formation of a carbonate mineral such as magnesite could be produced. The mineral carbonation is one of the potential strategies for CO_2 capture and storage processes.

Funding

This work was supported by Ministry of Science and Innovation, Spain, project PCI2019–111931-2 and the European Regional Development Fund (ERDF) - Next Generation / EU program.

CRediT authorship contribution statement

Celia Marcos: Conceptualization, Data curation, Formal analysis, Investigation, Methodology, Resources, Software, Supervision, Validation, Visualization, Writing – original draft, Writing – review & editing. **Ayoub Lahchich:** Investigation, Methodology, Software, Writing – original draft. **Pedro Álvarez-Lloret:** Conceptualization, Data curation, Formal analysis, Funding acquisition, Investigation, Methodology, Project administration, Resources, Software, Supervision, Validation, Visualization, Writing – review & editing.

Declaration of Competing Interest

The authors declare that they have no known competing financial interests or personal relationships that could have appeared to influence the work reported in this paper.

Data availability

Data will be made available on request. Data other than those presented in the article are available from the authors.

Acknowledgements

The authors wish to acknowledge the Scientific-Technical Services of the University of Oviedo (Spain) for X-ray diffraction, Thermogravimetric analyses and BET techniques.

References

Argüelles, A., Leoni, M., Blanco, J.A., Marcos, C., 2010. Semi-ordered crystalline structure of the Santa Olalla vermiculite inferred from X-ray powder diffraction. Am. Mineral. 95, 126–134.

Atilhan, M., Atilhan, S., Ullah, R., Anaya, B., Cagin, T., Yavuz, C.T., Aparicio, S., 2016. High-pressure methane, carbon dioxide, and nitrogen adsorption on amine-impregnated porous montmorillonite nanoclays. J. Chem. Eng. Data 61 (8), 2749–2760.

Barrett, E.P., Joyner, L.G., Halenda, P.P., 1951. The determination of pore volume and area distributions in porous substances. I. computations from nitrogen isotherms. J. Am. Chem. Soc. 73, 373–380.

Bassett, W.A., 1961. The geology of vermiculite occurrences. Clay Clay Miner. 10 (1), 61–69.

Bergaya, F., Lagaly, G., 2013. Some other materials related to clay minerals. Dev. Clay Sci. 5, 743.

Choi, H., Shin, J., Woo, J., 2018. Effect of electricity generation mix on battery electric vehicle adoption and it its environmental impact. Energy Policy 121, 13–24.

Chouikhi, N., Antonio, J., Vilarrasa, E., Besghaier, S., Chlendi, M., Rodriguez, F.E., Bagane, M., 2019. CO_2 adsorption of materials synthesized from clay minerals: a review. Materials 9, 514.

Churchman, G.J., Lowe, D.J., 2012. Alteration, formation, and occurrence of minerals in soils. In: Huang, P.M., Li, Y., Summer, M.E. (Eds.), Handbook of Soil Sciences, 2nd, Properties and Processes. CRC Press, Taylor and Francis, Boca Raton, FL, pp. 20.71–20.72.

Collins, M., Knutti, R., Arblaster, J., Dufresne, J.L., Fichefet, T., Friedlingstein, P., Gao, X., Gutowski, W.J., Johns, T., Krinner, G., Shongwe, M., Tebaldi, C., Weaver, A. J., Wehner, M., 2013. Long-term climate change: projections, commitments and irreversibility. In: Stocker, T.F., Qin, D., Plattner, G.K., Tignor, M., Allen, S.K., Boschung, J., Nauels, A., Xia, Y., Bex, V., Midgley, P.M. (Eds.), Climate Change 2013: The Physical Science Basis. Contribution of Working Group I to the Fifth Assessment Report of the Intergovernmental Panel on Climate Change. Cambridge University Press, Cambridge, United Kingdom and New York, NY, USA.

Couderc, P., Douillet, P., 1973. Les vermiculites industrielles: exfoliation, caractéristiques mineralogiques et chimiques. Bull. de la Soc. Francaise de Céramique 99, 51–59.

Daval, D., Martinez, I., Corvisier, J., Findling, N., Goffe, B., Guyot, F., 2009. Carbonation of Ca-bearing silicates, the case of wollastonite: experimental investigations and kinetic modeling. Chem. Geol. 265, 63–78.

de la Calle, C., Suquet, H., 1988. Vermiculite. In: Bailey, S.W. (Ed.), Hydrous Phyllosilicates. Reviews in Mineralogy, 19. Mineralogical Society of America, Washington, DC, pp. 455–496.

Faass, G.S., 1981. Correlation of Gas Adsorption, Mercury Intrusion, and Electron Microscopy Pore Property Data for Porous Glasses. Georgia Institute of Technology, p. 260.

Haque, E., Islam, M., Pourazadi, E., Sarkar, S., Harris, A.T., Minett, A.I., Yanmaz, E., Alshehri, S.M., Ide, Y., Wu, K.C., 2017. Boron functionalized graphene oxide-organic frameworks for highly eficient CO2 capture. Chem. Asian J. 12, 283–288.

Harvey, A., Boland, J.B., Godwin, I., Kelly, A.G., Szydłowska, B.M., Murtaza, G., Thomas, A., Lewis, D.J., O'Brien, P., Coleman, J.N., 2017. Exploring the versatility of liquid phase exfoliation: producing 2D nanosheets from talcum powder, cat litter and beach sand, 2D. Materials 4 (2), 25–54.

Hillier, S., Marwa, E.M.M., Rice, C.M., 2013. On the mechanism of exfoliation of vermiculite. Clay Miner. 48, 563–582.

Inguanzo, M., Menéndez, J.A., Fuente, E., Pis, J.J., 2001. Reactivity of pyrolyzed sewage sludge in air and CO2. J. Anal. Appl. Pyrolysis 58-59, 943–954.

Kabir, E., Kumar, P., Kumar, S., Adelodun, A.A., Kim, K.-H., 2018. Solar energy: potential and future prospects. Renew. Sust. Energ. Rev. 82, 894–900.

Lackner, K.S., Butt, D.P., Wendt, C.H., 1997. Progress on binding CO_2 in mineral substrates. Energy Convers. Manag. 38, 259–264.

Lan, X., Hall, B.D., Dutton, G., Mühle, J., Elkins, J.W., 2020. Atmospheric composition. In State of the Climate in 2018, Chapter 2: Global Climate. Spe. Online Suppl. Bull. American Meteorol. Soc. 101 (8). August, 2020.

Li, G., Xiao, P., Webley, P., Zhang, J., Singh, R., Marshall, M., 2008. Capture of CO_2 from high humidity flue gas by vacuum swing adsorption with zeolite 13X. Adsorption 14, 415–422.

Marcos, C., 2020. Structural changes in vermiculites induced by temperature, pressure, irradiation, and chemical treatments. In: Nascimento, G.M.D. (Ed.), Clay Science and Technology. IntechOpen, London. https://doi.org/10.5772/intechopen.92436.

Marcos, C., 2022. Effect of water immersion on raw and expanded ugandan vermiculite. Minerals 12 (1), 23.

Marcos, C., Rodriguez, I., 2016. Structural changes on vermiculite treated with methanol and ethanol and subsequent microwave irradiation. Appl. Clay Sci. 123, 304–314.

Marcos, C., Rodriguez, I., 2017. Effect of propanol and butanol and subsequent microwave irradiation on the structure of commercial vermiculites. Appl. Clay Sci. 144, 104–114.

Marcos, C., Arango, Y.C., Rodríguez, I., 2009. X-ray diffraction studies of the thermal behaviour of commercial vermiculites. Appl. Clay Sci. 42, 368–378.

Marcos, C., Medoro, V., Adawy, A., 2020. Modified vermiculite as adsorbent of hexavalent chromium in aqueous solution. Minerals 10 (9), 749.

Midgley, H.G., Midgley, C.M., 1960. The mineralogy of some commercial vermiculites. Clay Miner. Bull. 23, 142–150.

Mohammed, I.J., Al-Mashaikie, S.Z., 2018. Origin and distribution of clay minerals in the mudstones of the Kolosh formation in Rawandoz area, North-eastern Iraq. Iraqi Geol. J. 51 (2), 75–90.

[NASA Global Climate Change, 2022. Vital Signs of the Planet: Carbon Dioxide. https://climate.nasa.gov/vital-signs/carbon-dioxide/.

Pera-Titus, M., 2014. Porous inorganic membranes for CO2 capture: present and prospects. Chem. Rev. 114, 1413–1492.

Pereira, M.H.S., dos Santos, C.G., de Lima, G.M., Oliveira-Bruziquesi, C.G., de Alvarenga-Oliveira, V., 2022. Capture of CO2 by vermiculite impregnated with CaO. Carbon Manag. 13 (1), 117–126.

Pevida, C., Plaza, M.G., Arias, B., Fermoso, J., Rubiera, F., Pis, J.J., 2008. Surface modification of activated carbons for CO_2 capture. Appl. Surf. Sci. 254, 7165–7172.

Rahman, F.A., Aziz, M.M.A., Saidur, R., Bakar, W.A., Hainin, M.R., Putrajaya, R., et al., 2017. Pollution to solution: capture and sequestration of carbon dioxide (CO_2) and its utilization as a renewable energy source for a sustainable future. Renew. Sust. Energ. Rev. 71, 112–126.

Roy, R., Romo, L.A., 1957. Weathering studies. I. New data on vermiculite. J. Geol. 66, 603.

Sanna, A., Uibu, M., Caramanna, G., Kuusik, R., Maroto-Valer, M.M., 2014. A review of mineral carbonation technologies to sequester CO2. Chem. Soc. Rev. 43, 8049–8080.

Sanz-Pérez, E.S., Arencibia, A., Calleja, G., San, R., 2018. Tuning the textural properties of HMS mesoporous silica. Functionalization towards CO_2 adsorption. Microporous Mesoporous Mater. 260, 235–244.

Seifritz, W., 1990. CO2 disposal by means of silicates. Nature 345, 486.

Sordakis, K., Tang, C., Vogt, L.K., Junge, H., Dyson, P.J., Beller, M., Laurenczy, G., 2018. Homogeneous catalysis for sustainable hydrogen storage in formic acid and alcohols. Chem. Rev. 118 (2), 372–433.

Thommes, M., Kaneko, K., Neimark, A.V., Olivier, J.P., Rodriguez-Reinoso, F., Rouquerol, J., Sing, K.S.W., 2015. Physisorption of gases, with special reference to the evaluation of surface area and pore size distribution (IUPAC Technical Report). Pure Appl. Chem. 87 (9–10), 1051–1069.

Toksoy-Koksal, F., Turkmenoglu, A.G., Goncuoglu, M.C., 2001. Vermiculitization of Phlogopite in metagabbro, Central Turkey. Clay Clay Miner. 49 (1), 81–91.

Velde, B., 1978. High temperature or metamorphic vermiculites. Contrib. Mineral. Petrol. 66, 319–323.

Wang, W.L., Xiao, J., Wei, X.L., Ding, J., Wang, X.X., Song, C.S., 2014. Development of a new clay supported polyethylenimine composite for CO2 capture. Appl. Energy 113, 334–341.

Yang, H., Xu, Z., Fan, M., Guptaa, R., Slimanec, R., Bland, A., 2008. Progress in carbon dioxide separation and capture: a review. Environ. Sci. 20, 14–27.

Zhang, Y., Chen, M., Li, G., Shi, Ch., Wang, B., Ling, Z., 2020. Exfoliated vermiculite nanosheets supporting tetraethylenepentamine for CO2 capture. Materials 7, 100–102.